PHYSICAL REVIEW A **93**, 050502(R) (2016)

Fano resonances observed in helium nanodroplets

A. C. LaForge,[1,*] D. Regina,[1] G. Jabbari,[2] K. Gokhberg,[2] N. V. Kryzhevoi,[2] S. R. Krishnan,[3] M. Hess,[1] P. O'Keeffe,[4] A. Ciavardini,[4] K. C. Prince,[5] R. Richter,[5] F. Stienkemeier,[1] L. S. Cederbaum,[2] T. Pfeifer,[6] R. Moshammer,[6] and M. Mudrich[1]

[1]*Physikalisches Institut, Universität Freiburg, 79104 Freiburg, Germany*
[2]*Physikalisch-Chemisches Institut, Universität Heidelberg, 69120 Heidelberg, Germany*
[3]*Department of Physics, Indian Institute of Technology–Madras, Chennai 600 036, India*
[4]*CNR–Istituto di Struttura della Materia, CP10, 00016 Monterotondo Scalo, Italy*
[5]*Elettra-Sincrotrone Trieste, 34149 Basovizza, Trieste, Italy*
[6]*Max-Planck-Institut für Kernphysik, 69117 Heidelberg, Germany*

(Received 24 November 2015; published 10 May 2016)

Doubly excited Rydberg states of helium (He) have been studied in nanodroplets using synchrotron radiation. Although qualitatively similar to their atomic counterparts, the Fano resonances in droplets are broader and exhibit blueshifts which increase for the higher excited states. However, varying the droplet size hardly affects the shapes of the resonances. Furthermore, additional dipole-forbidden resonances appear which are not seen in the He atom. We discuss these features in terms of localized atomic states perturbed by the surrounding He atoms.

DOI: 10.1103/PhysRevA.93.050502

Electronic correlation is of fundamental importance in atomic and molecular systems. In particular, the interaction of energetic photons with many-electron systems is governed by electron correlation leading to processes such as shake-off in single photon double ionization [1], post collision interaction in Auger processes [2], and autoionization of doubly excited states [3]. Furthermore, the presence of weakly bound neighboring atoms opens additional correlated decay channels such as interatomic Coulombic decay (ICD) [4], a fertile area of research in recent years. Even for the He dimer, in which the He atoms are separated by 52 Å in the ground state, correlation-induced decay via ICD was recently observed [5,6].

Generally speaking, electronically excited free atoms and small molecules exhibit a wealth of fine structure in their Rydberg and double excitation spectra, while in condensed matter these structures tend to be unresolved or simply vanish. The reason is that the wave functions of excited atoms are spatially extended and thus experience strong perturbations by neighboring atoms when localized in a condensed phase system. The confinement of the excited state orbital causes substantial energy shifts, and in ordered systems singly excited states evolve into excitons (e.g., [7,8]). Doubly excited states occupy a special place in the study of electronic structure since they are characterized by a high degree of electron correlation. As they comprise two electrons excited by a single photon, they are expected to be more sensitive to perturbation by the environment.

As originally described by Fano, the interference of a discrete autoionizing state with a continuum gives rise to a characteristically asymmetric peak in the excitation spectrum [9]. In the case of double excitation of He, the Rydberg series converging to the $N = 2$ threshold interacts with the continuum above the $N = 1$ ionization threshold of He. This results in the well-known Fano profile of the cross section [10],

$$\sigma(E) = \sigma_a \frac{(q+\epsilon)^2}{(1+\epsilon^2)} + \sigma_b, \quad \text{where } \epsilon = \frac{E - E_0}{\Gamma/2} \qquad (1)$$

is the reduced energy, E_0 is the resonance energy, Γ is the linewidth of the resonance, and q^2 represents the ratio of the transition probabilities to the discrete state and to the continuum ("Fano q parameter"). σ_a is the background cross section associated with the fraction of the ionization continuum with which the discrete state interferes, while σ_b is the noninterfering background cross section. An excellent overview is given by Rost *et al.* [11].

For rare gas clusters and condensed neon, broad features were observed near the well-known atomic window resonances [3]. They were attributed to surface and bulk excitations, but the assignment of the features has remained tentative [12–16]. He droplets offer a unique system of an extremely weakly bound van der Waals superfluid with a homogeneous density distribution [17]. He is the simplest paradigm system to study double excitations [9] and has the advantage that it is also amenable to accurate model calculations [18].

In this Rapid Communication, we report the resonant double excitation of He atoms in nanodroplets, measured by XUV synchrotron radiation. In contrast to a recent series of experiments where many atoms in the droplet were resonantly excited by intense XUV radiation [19,20], here, the excitation is confined to a single atom within the droplet and Fano profiles similar to those of atomic He are observed. The significant broadening and shifting of the droplet resonances is discussed below in the context of perturbed localized states in the clusters.

The experiment was performed using a mobile He droplet source attached to an imaging photoelectron-photoion coincidence (PEPICO) detector at the GasPhase beamline of Elettra-Sincrotrone Trieste, Italy. The setup has been described in some detail earlier [21,22] and only the relevant parts are described here. A beam of He nanodroplets is produced by

*aaron.laforge@physik.uni-freiburg.de

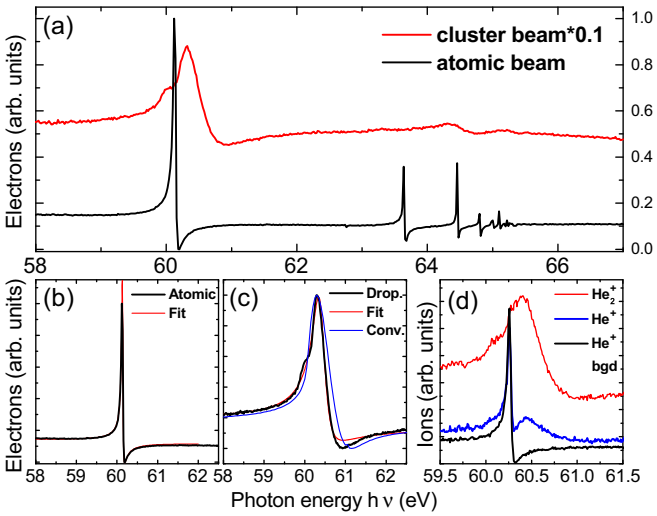

FIG. 1. (a) Electron signals of He atoms at a nozzle temperature of $T = 40$ K [black (lower) line] and of He droplets [red (upper) line] consisting of 10^9 He atoms ($T = 8$ K) as a function of the photon energy. (b) Fano profile fit (red) to the $2s2p+$ resonance of the atomic resonance signal (black). (c) Fano profile fit (red) to the droplet equivalent of the $2s2p+$ resonance (black). The blue line shows the convolution of the atomic $2s2p+$ resonance with the line profile of the singly excited $1s2p$ droplet line shape from Ref. [8]. (d) He^+ and He_2^+ ions yield spectra recorded at $T = 17$ K ($\langle N \rangle \approx 7000$). The black (lower) line depicts the He^+ yield from the He background (chopper closed), the blue (middle) line shows the He^+ yield from the droplet beam with background subtraction (chopper open − closed), and the red (upper) line shows the He_2^+ yield from the droplet beam with background subtraction (chopper open − closed).

continuously expanding high purity He (50 bar, purity He 6.0) out of a cold nozzle ($T = 40 - 7$ K) of diameter 5 μm into vacuum. Under these expansion conditions, the mean droplet sizes range from 1 to 10^{10} He atoms per droplet [23]. After passing a skimmer (0.4 mm) and a mechanical beam chopper for discriminating the droplet beam signal from the He background, the He droplet beam next crosses the synchrotron beam inside a PEPICO detector consisting of an ion time-of-flight detector and a velocity map imaging detector operating in coincidence. For the experiments reported in this work, only the electron and mass-gated ion signals were measured for photon energies below the double ionization threshold ($h\nu = 58$–68 eV) [3]. The photon energy was scanned with a typical step size of 20 meV and an energy resolution $E/\Delta E \approx 10^4$ by simultaneously varying the undulator gap and monochromator. The peak intensity in the interaction region was estimated to be around 15 W/m^2. The intensity of the radiation was monitored by a calibrated photodiode and all photon-energy-dependent ion and electron spectra shown in this work are normalized to this intensity.

Figure 1(a) shows the total electron yield from an atomic He beam [$T = 40$ K, black (lower) line], and from a droplet beam with $\langle N \rangle \approx 10^9$ [$T = 8$ K, red (upper) line]. The intensity of the atomic beam was normalized to unity while the droplet beam intensity was normalized by the same factor along with an additional factor of 0.1 to improve visibility. For the atomic beam, we observe the resonance lines previously reported [3,10]. Here we will only use their well-known resonance energies and shapes as references. In comparison, the droplet resonances are significantly broadened and upshifted in energy.

When we record the yield of He^+ ions instead of electrons, mainly the sharp atomic lines are seen, whereas the He_2^+-specific spectra show only the broadened profiles [see Fig. 1(d)]. The deviation of the droplet beam-correlated He^+ signal which is most pronounced around the maximum of the He_2^+ yield seems to result from a contribution of a fraction of the He_2^+ signal to the He^+ yield, possibly due to fragmentation. Due to its close proximity to the atomic resonance, we attribute the broad feature around $h\nu = 60.4$ eV to the droplet equivalent of the $2s2p+$ state. For a more quantitative analysis we fit both the atomic and droplet resonances with Eq. (1) [red lines in Figs. 1(b) and1(c)]. From the fit, we find the resonance energy and width for the droplet to be 60.4 eV and 420 meV, respectively, while the q parameter is -2.36. In comparison, the resonance energy, width, and q parameter for the corresponding atomic resonances are 60.15, 37 meV, and -2.77, respectively [10]. Thus, the droplet resonance is blueshifted by about 300 meV, the width is much larger, while the q parameter is only slightly lower.

Similar line broadenings and shifts were previously observed for single excitations of He droplets by Joppien *et al.* [8]. In that work, fluorescence spectra of He clusters were measured for photon energies $h\nu = 20$–25 eV. The observed band structures were compared to absorption lines of heavier rare-gas clusters [24] which were explained in terms of the Frenkel or Wannier exciton model. However, exciton models failed for He droplets. The interpretation given by Joppien *et al.* in terms of perturbed localized excited atoms instead of excitons as in heavier rare-gas clusters is mainly based on the low density as well as the low dielectric constant of liquid He. Since the exciton radius for the lowest singly excited states is smaller than the nearest-neighbor (nn) distance in the droplet, the line shift is caused by the repulsive interaction between the excited electron and the surrounding He environment. Recently, the simple model of Kornilov *et al.* [25] based on atomic Rydberg states perturbed by the mean field of the surrounding He gave good agreement with experiment. As an attempt to relate the observed line broadening of doubly excited states to the single excitation features we convolute the atomic $2s2p+$ resonance with the line profile of the singly excited $1s2p$ state of the droplet from Ref. [8] and compare with the droplet $2s2p+$ resonance for $\langle N \rangle \approx 10^9$ in Fig. 1(c). The good agreement gives a first indication that the observed line profile of doubly excited He droplets can be attributed to similar perturbations of the localized excited atom by the surrounding ground state He as in singly excited droplets.

In Fig. 2(a), the electron signals are plotted for droplet sizes ranging from $\langle N \rangle \approx 1$ up to 10^{11} atoms in the full range of measured photon energies. In contrast to atomic resonances which feature vanishing signal at the minima of the Fano profiles, the droplet resonances show a large background signal on which the profile resides. For the atomic case, the decay mechanisms are limited to either autoionization or the slower fluorescence decay [26], resulting in a nearly perfect contrast in the interference between direct ionization and autoionization. Droplets, on the other hand, exhibit a

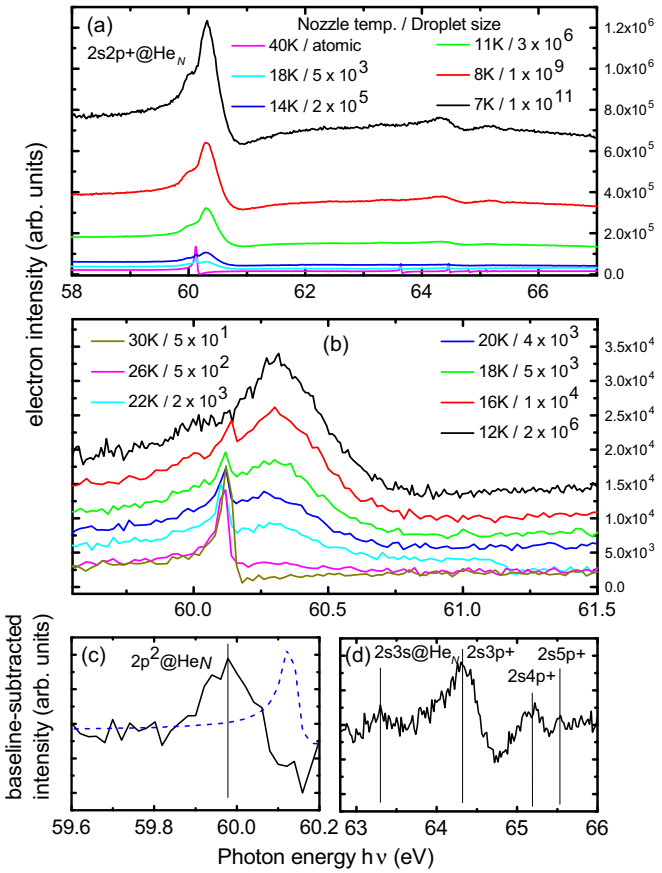

FIG. 2. (a) Electron-yield spectra at various nozzle temperatures corresponding to gas phase atoms and nanodroplets of various sizes. (b) Electron-yield spectra centered at the $2s2p+$ resonance. (c) and (d) Baseline-subtracted electron signals for a droplet size of 10^{11} atoms (7 K) for selected energy ranges along with the atomic $2s2p+$ resonance (blue dashed line).

weaker interference contrast, presumably due to the presence of additional decay mechanisms. Besides the aforementioned decay channels, ICD is energetically allowed [6] and direct ionization of closely spaced He atoms forming He dimer, trimer, and higher oligomer ions also contributes [27].

While the repulsive interactions between a localized excited He atom and its environment appear to be at the origin of the observed droplet features, the role of inhomogeneous broadening due to the density variation at the droplet surface may play a role. Figure 2(b) shows the $2s2p+$ resonance for sizes from single He atoms to large clusters. For small clusters, $\langle N\rangle \leqslant 500$ at $T \geqslant 26$ K, the Fano profiles are nearly identical in terms of line shape and width to the pure atomic line. This can be explained by the large atomic contribution to the droplet beam. When lowering the nozzle temperature to increase the droplet fraction and size, the broadened Fano profile starts to appear already with nearly identical parameters to those of the larger droplets (Fig. 1) when the atomic profile is subtracted. At a nozzle temperature $T = 22$ K (mean droplet size $\langle N\rangle \approx 2000$) we find $E_0 = 60.39$ eV, $\Gamma = 400$ meV, and $q = -2.2$. As the average size of the nanodroplets increases, the broadened Fano profile becomes the dominant feature in the spectra, even superseding the atomic profile at $\langle N\rangle \approx 2\times10^6$ ($T = 12$ K). The surprising observation that the shape of the resonance profile remains nearly constant, irrespective of the strongly changing ratio of surface to bulk regions of the droplets for the varying droplet size, indicates that inhomogeneous broadening is negligible. On the contrary, the observed profile can be regarded as the characteristic line shape of bulk superfluid He which is dominated by homogeneous broadening as discussed above.

This interpretation is supported by the observed qualitative difference between the He^+ and $He_2{}^+$ ion yield spectra [Fig. 1(d)]. The $He_2{}^+$ signal can be clearly associated with ionization processes taking place in the bulk of the droplets, as has been discussed previously [28]. The He^+ signal mostly stems from ionized free He atoms accompanying the droplet beam. The fact that the atomic Fano profile is overlapped by a weak contribution of the broadened droplet contour points to fragmentation of $He_2{}^+$ formed in highly excited vibrational states adding to the He^+ signal. Surprisingly, again no increase of the width of the Fano profiles is seen in the He^+ nor in the $He_2{}^+$ signal for any droplet size.

For droplet sizes $\langle N\rangle \geqslant 3\times10^7$ atoms ($T \leqslant 11$ K) and greater, additional Fano resonances appear at higher photon energies in Fig. 2(a). To isolate these profiles as well as any additional features, we fit the background signal with a low-order polynomial, and perform a baseline subtraction for a droplet size of 10^{11} atoms. Figures 2(c) and 2(d) show the baseline-subtracted electron intensities for the photon energy ranges of 59.6–60.2 eV and 62.8–66 eV, respectively. Figure 2(c) additionally includes the atomic $2s3p+$ resonance (blue dotted line) due to its close proximity to the possible droplet resonance. Black vertical lines indicate the energies of possible resonances. The most prominent features are the three sequential resonances at 64.3, 65.2, and 65.5 eV (peak positions). These are assigned to the higher members of the $2snp+$ series. Compared to the blueshift observed in singly excited droplets [8] and the $2s2p+$ droplet resonance, the states with higher quantum numbers exhibit a much larger shift in energy [about 720(40) meV for the droplet $2s3p+$ resonance and about 815(50) meV for the droplet $2s4p+$ and $2s5p+$ resonances of a droplet consisting of 10^{11} atoms]. In line with our interpretation of the shifted and broadened droplet resonances, the larger blueshift for higher quantum numbers is due to a larger orbital radius which then implies a stronger repulsion from the surrounding He. Note that there are two additional peaks at about 60.0 and 63.3 eV [Figs. 2(c) and 2(d)]. Given the symmetry breaking induced by the He droplet environment, additional dipole-forbidden atomic resonances may become allowed in the droplet. To exclude the possibility that the resonance at 60.0 eV is simply an artifact from the subtraction of the atomic resonance at 60.1 eV, the atomic spectrum is included in Fig. 2(c).

Fully quantum mechanical model calculations on large-scale systems such as nanodroplets are challenging, while *ab initio* calculations on simpler systems (e.g., dimers) can give insight into the effect of formation of complexes on the electronic properties of doubly excited atoms. Thus, we calculated the potential energy curves for He dimers for the lower doubly excited states, shown in Fig. 3 along with the nearest neighbor (nn) distribution (bottom) for He droplets [27]. We employed an algebraic diagrammatic construction (ADC) method for the

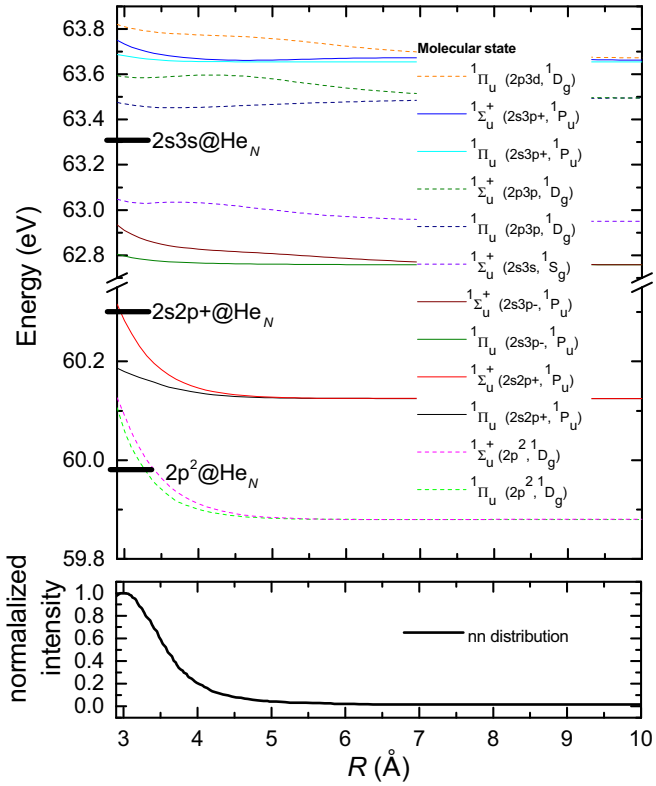

FIG. 3. Computed excitation energies for doubly excited resonances accessible in dipole transitions of the He dimer (top) along with the nearest neighbor (nn) distribution (bottom) for He droplets (taken from [27]). The excited states correlated with the dipole-allowed transitions in the He atom are plotted as solid lines, and the dipole-forbidden transitions as dashed lines. The first three droplet resonances are marked as thick tick marks on the y axis.

polarization propagator [29,30]. In particular, we projected the electronic Hamiltonian onto the space of the two-hole–two-particle ($2h2p$) configurations and diagonalized it to obtain the discrete parts of Fano resonances. The *ab initio* calculations were carried out using a cc-pV6Z basis set on the He atoms augmented by five s-type, five p-type, and three d-type and seven s-type, six p-type, and five d-type even-tempered ($\beta = 2.5$) Gaussian-type functions for the $2s2p$ and $2s3p$ resonances, respectively. The g-, and h-type functions were removed from the underlying basis set, since their influence on the excitation energies of the considered states was found to be negligible. The MOLCAS 7.4 package [31] was employed for the *ab initio* calculation of two-electron integrals and one-particle transition dipole moments needed for ADC.

For comparison, the peak positions of the first three droplet resonances are added as tick marks on the vertical scale. Overall, the $n = 2$ droplet resonances are consistent with the blueshift expected from the model excitation energies considering vertical transitions at the He-He nn distance ($\sim$3 Å) in droplets. The peak at 60.0 eV corresponds most likely to the dipole-forbidden $2p^2$ state and the peak at 63.3 eV to the dipole-forbidden $2s3s$ state. The $2s2p+$ state is blueshifted further than the $2p^2$ state but still roughly matches the calculated potential curve. The splitting and shifting of the excitation energy along with the broad nn distribution therefore

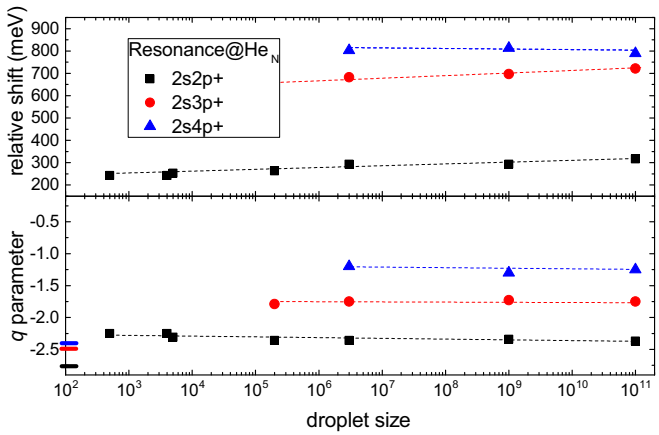

FIG. 4. Droplet-size dependence of the shift of the droplet resonance with respect to the atomic line (a) and the Fano q parameter (b) for the first three resonances of the $2snp+$ series. Dashed lines are linear fits to guide the eyes. The respective atomic q parameters are shown as colored tick marks on the y axis.

partially explain the observed broadening and blueshifting of the resonance profiles. For the $n = 3$ states the droplet resonances exhibit a stronger blueshift than predicted by the excitation energies due to the breakdown of the model of a localized excitation, which makes the assignment more uncertain. The good agreement between observed line shifts and the computed excitation energies for the low-lying states support our interpretation in terms of repulsive interaction between localized excited states and the nearest neighboring He atoms.

Finally, we summarize in Fig. 4(a) the shifts of droplet resonances with respect to the atomic resonance, and in Fig. 4(b) the values of the q parameter for the first three resonances of the $2snp+$ series as a function of the droplet size. The resonances were fitted using Eq. (1) and the values given correspond to the resonance energy, E_0. All three resonances have widths close to that of the droplet $2s2p+$ feature [400(50) meV], however, their respective q parameters drop to -1.75 for the droplet $2s3p+$ resonance and to -1.25 for the droplet $2s4p+$ resonance. The $2s2p+$ resonance shows a slight droplet-size dependence of the line shift, whereby smaller droplets are closer to the atomic resonance. The higher resonances show no such dependence within the limited statistics of the weak signals. The q parameter appears to be constant over the entire droplet size range for all resonances suggesting no change in the relative transition amplitudes for excitation, ionization, and autoionization with droplet size.

In conclusion, we have observed autoionizing doubly excited resonances in van der Waals-bonded He nanodroplets along with corresponding Fano profiles when scanning over the resonance energies. Relative to the atomic lines, the droplet resonances are significantly broadened and blueshifted similar to features seen in singly excited droplets [8] due to the localized doubly excited He atoms being perturbed by the neighboring droplet environment. Furthermore, a clear size dependence is observed in the overall electron intensity such that the strongest Fano profiles occur for droplets consisting of 10^6–10^{11} atoms; however, the linewidths and Fano q

parameters show little to no droplet-size dependence leading one to conclude that the excitation/ionization mechanisms do not depend on droplet size but are characteristic for bulk superfluid He.

Possible directions for future research include measuring Fano resonances using size-selected He_2, He_3, and other small clusters, e.g., to scrutinize the model potentials presented here. Furthermore, the role of ICD in the decay of doubly excited states in the clusters could be ascertained by means of ion mass-correlated photoelectron spectroscopy. In general, an accurate theoretical model for electronic excitation spectra in He droplets is still lacking. In this regard, the present data may help to establish a better understanding of the droplet-induced perturbation of excited states due to the additional degree of freedom of autoionization which is incorporated in the q parameter.

The authors gratefully acknowledge the staff of 328 Elettra-Sincrotrone Trieste for providing high-quality light. A.C.L., D.R., M.H., and M.M. gratefully acknowledge the financial support of Deutsche Forschungsgemeinschaft (DFG) (Grant No. MU 2347/10-1). N.V.K., K.G., and L.S.C. gratefully acknowledge the financial support of DFG (research unit 1789). G.J. thanks IMPRS-QD for financial support.

[1] T. Pattard, T. Schneider, and J. Rost, J. Phys. B: At., Mol. Opt. Phys. **36**, L189 (2003).
[2] A. Russek and W. Mehlhorn, J. Phys. B: At., Mol. Opt. Phys. **19**, 911 (1986).
[3] R. Madden and K. Codling, Phys. Rev. Lett. **10**, 516 (1963).
[4] L. S. Cederbaum, J. Zobeley, and F. Tarantelli, Phys. Rev. Lett. **79**, 4778 (1997).
[5] N. Sisourat, N. V. Kryzhevoi, P. Kolorenč, S. Scheit, T. Jahnke, and L. S. Cederbaum, Nat. Phys. **6**, 508 (2010).
[6] T. Havermeier *et al.*, Phys. Rev. Lett. **104**, 133401 (2010).
[7] J. Wörmer, M. Joppien, G. Zimmerer, and T. Möller, Phys. Rev. Lett. **67**, 2053 (1991).
[8] M. Joppien, R. Karnbach, and T. Möller, Phys. Rev. Lett. **71**, 2654 (1993).
[9] U. Fano, Phys. Rev. **124**, 1866 (1961).
[10] M. Domke, K. Schulz, G. Remmers, G. Kaindl, and D. Wintgen, Phys. Rev. A **53**, 1424 (1996).
[11] J. M. Rost, K. Schulz, M. Domke, and G. Kaindl, J. Phys. B: At., Mol. Opt. Phys. **30**, 4663 (1997).
[12] R. Müller, M. Joppien, and T. Möller, Z. Phys. D: At., Mol. Clusters **26**, 370 (1993).
[13] R. Thissen, P. Lablanquie, R. Hall, M. Ukai, and K. Ito, Eur. Phys. J. D **4**, 335 (1998).
[14] A. Pavlychev and E. Rühl, J. Electron. Spectrosc. Relat. Phenom. **106**, 207 (2000).
[15] H. Zhang, D. Rolles, J. D. Bozek, and N. Berrah, J. Phys. B: At., Mol. Opt. Phys. **42**, 105103 (2009).
[16] B. Kassühlke and P. Feulner, Low Temp. Phys. **38**, 749 (2012).
[17] J. P. Toennies and A. F. Vilesov, Angew. Chem., Int. Ed. **43**, 2622 (2004).
[18] A. Burgers, D. Wintgen, and J.-M. Rost, J. Phys. B: At., Mol. Opt. Phys. **28**, 3163 (1995).
[19] A. C. LaForge *et al.*, Sci. Rep. **4**, 3621 (2014).
[20] Y. Ovcharenko *et al.*, Phys. Rev. Lett. **112**, 073401 (2014).
[21] P. O'Keeffe *et al.*, Rev. Sci. Instrum. **82**, 033109 (2011).
[22] D. Buchta *et al.*, J. Phys. Chem. A **117**, 4394 (2013).
[23] L. F. Gomez, E. Loginov, R. Sliter, and A. F. Vilesov, J. Chem. Phys. **135**, 154201 (2011).
[24] N. Schwentner, E.-E. Koch, and J. Jortner, in *Electronic Excitations in Condensed Rare Gases*, Springer Tracts in Modern Physics Vol. 107 (Springer-Verlag, Berlin, 1985), p. 1.
[25] O. Kornilov *et al.*, J. Phys. Chem. A **115**, 7891 (2011).
[26] F. Penent *et al.*, Phys. Rev. Lett. **86**, 2758 (2001).
[27] D. S. Peterka *et al.*, J. Phys. Chem. A **111**, 7449 (2007).
[28] D. Buchta *et al.*, J. Chem. Phys. **139**, 084301 (2013).
[29] J. Schirmer, Phys. Rev. A **26**, 2395 (1982).
[30] S. Kopelke, K. Gokhberg, V. Averbukh, F. Tarantelli, and L. Cederbaum, J. Chem. Phys. **134**, 094107 (2011).
[31] F. Aquilante *et al.*, J. Comput. Chem. **31**, 224 (2010).